



# The influence of different crystal modifiers on ultra-low embodied energy curing fiber-reinforced cement composites

Passakorn SONPRASARN<sup>1</sup>, Wichit PRAKAYPAN<sup>2</sup>, Sureerat POLSILAPA<sup>1</sup>, Nuntaporn KONGKAJUN<sup>3</sup>, Edward A. LAITILA<sup>4</sup>, Nutthita CHUANKRERKKUL<sup>5</sup>, and Parinya CHAKARTNARODOM<sup>1,\*</sup>

<sup>1</sup> Department of Materials Engineering, Faculty of Engineering, Kasetsart University, Ngamwongwan Road, Chatuchak, Bangkok, 10900, Thailand

<sup>2</sup> UAC Global Public Company Limited, Vibhavadirangsit Road, Chatuchak, Bangkok 10900, Thailand

<sup>3</sup> Department of Materials and Textile Technology, Faculty of Science and Technology, Thammasat University, Paholyothin Road, Klong Luang, Pathumthani, 12120, Thailand

<sup>4</sup> Department of Materials Science and Engineering, Michigan Technological University, Townsend Drive, Houghton, MI, 49931, USA

<sup>5</sup> Metallurgy and Materials Science Research Institute, Chulalongkorn University, Soi Chulalongkorn 12, Patumwan, Bangkok, 10330, Thailand

\*Corresponding author e-mail: fengpryc@ku.ac.th

## Received date:

4 June 2022

## Revised date

12 September 2022

## Accepted date:

18 September 2022

## Keywords:

Fiber cement;  
Tobermorite;  
Moisture curing;  
Hydration reaction;  
Low embodied energy

## Abstract

Fiber-reinforced cement composites (FRCC) are widely used in the construction of houses and commercial buildings in many countries such as the United States, the United Kingdom, the European countries, and the Asian countries such as China, India, and Thailand. Conventionally, the FRCC is manufactured from Portland cement, silica sand, and cellulose fiber using the so-called autoclaved curing under a designate hydrothermal condition to accelerate the hydration reaction resulting in superior properties. However, the autoclave-curing process needs a huge investment and generates highly environmental impact specially greenhouse gases due to its heavy energy consumption. Hence, this research aims to develop the FRCC with lowering embodied energy via the energy-free moisture curing process. The use of different crystal modifiers (CM) including synthetic tobermorite, aluminosilicate complex, and modified lithium compound in addition of the usual FRCC composition to drive the hydration kinetic and then properties achieved were characterized by the relevance of higher heat of hydration. Moreover, scanning electron microscope (SEM) were used to reveal the favorable effects of appropriate CM through the microstructure. The results approved that the FRCC with qualified mechanical performance and densified microstructure was successfully produced by using the appropriate moisture curing condition and CM. Additionally, using aluminosilicate complex as CM at 3% of cement weight produced FRCC with the highest modulus of elasticity of  $9,067 \pm 492$  MPa, and the lowest % water absorption of  $27.42 \pm 1.65$  %.

## 1. Introduction

During the 2021 united nations climate change conference (COP 26), many countries including Thailand announced their target for net zero greenhouse gas emissions by the year 2050 [1]. Manufacturing sector is important for the national economy. However, the chemical and physical processes used to transform raw materials into the products can generate numerous greenhouse gases such as carbon dioxide (CO<sub>2</sub>), methane (CH<sub>4</sub>), nitrous oxide (N<sub>2</sub>O), hydrofluorocarbons (HFCs) and perfluorocarbons (PFCs). Based on the 2006 intergovernmental panel on climate change (IPCC) guidelines for national greenhouse gas inventories, the manufacturing sector is in the group of manufacturing processes and product uses. In 2017, Thai industries within this group released 19,178.44 GgCO<sub>2</sub>eq of greenhouse gas, and about 96% was from cement production leading to a high carbon-footprint in the cement-based construction materials [2,3]. According to Vallejo *et al* [4], about 40% of carbon-footprint generated from construction activities was from the cement-based construction materials used in the construction

project. Therefore, reduction of carbon-footprint in cement-based construction materials will significantly reduce the carbon-footprint and help support the goal of net zero emissions by 2050.

Using recycled materials is an approach to reduce the carbon-footprint in construction materials and can gain other benefits. Kongkajun *et al* [5] studied the recycling of wastes from brick and fiber-cement factories. The results showed that both industrial wastes could be used as the partial replacement of Portland cement, laterite, and sand used to produce soil-cement bricks. In addition, by using both wastes, there was a reduction of thermal conductivity and density of the bricks. Reduction of the thermal conductivity improves the insulative properties of the bricks, reducing building energy requirements and the greenhouse gas emissions from the heating/cooling processes. As for the reduction of the density, the reduced weight would reduce the fuel consumption and thus greenhouse gas emissions during the transportation per brick.

Fiber cement or fiber-reinforced cement composites (FRCC) are composite materials commonly used in the construction of houses and

commercial buildings. This group of materials are used for interior and exterior applications such as roofing, wall, cladding, lining and flooring. General properties of FRCC are higher strength, durable, pest and fire resistance. Currently, FRCC are manufactured from natural raw materials consisting of ordinary Portland cement (OPC), sea sand, gypsum, cellulose fiber. According to our previous works, coal-fired bottom ash treated with the chemical admixture could fully replace the sand used in FRCC production [6,7]. Also, from our previous work, gypsum in FRCC was replaced with the fiber-cement waste treated chemical admixture. For the latter work, it reduces not only carbon-footprint of the FRCC but also fiber-cement waste management cost incurred by the factory [8,9].

Of course, recycling is a common method for carbon-footprint reduction. To further reduce carbon-footprint, reduction in energy usage in the manufacturing process is another approach. For the manufacturing process of FRCC, the raw materials are mixed with water and then molded by the process, such as the Hatschek process, filter pressing process, or flow-on process. After molding, the green sheets of FRCC are cured.

Generally, curing is a process of providing the adequate moisture to the cement-based materials allowing the hydration reaction between OPC and water to continue constantly. Normally, the curing process could take 28 days. To accelerate the process, moisture curing (also known as steam curing) may be employed to increase the strength of cement-based materials at the early stage. For this process, the material is kept in the high humidity chamber at atmospheric pressure and temperature between 40°C to 80°C for a period of time [10,11].

In FRCC industry, autoclave curing is a common curing process used to accelerate the hydration reaction. In this process, the green FRCC sheets are cured in the autoclaved about 1 day at the temperature between 160°C to 180°C and the pressure between 8 bars to 12 bars. The 28-days strength by normal curing for FRCC sheets could be achieved after autoclave curing. Even though the FRCC cured by the autoclave has desirable properties, this requires a high capital investment for the machines and the energy used during the operation [12-17].

The chemical admixture is a material that, when it is added to concrete or mortar, can improve some properties such as strength, durability, hydration reaction rate, and setting time of cement. The examples are the lithium compounds and zeolite that can improve the properties of both concrete and FRCC such as strength, micro-structure, water absorption, and freeze-thaw cycle resistance [15,18-25]. Alumino-silicate material is an admixture that has the pozzolanic property. When it is added to the concrete, it improves early strength development while also reducing the setting time. Moreover, the resistance to freeze-thaw cycle, chloride attack, and sulfate attack are also improved [26,27].

**Table 1.** Chemical composition of raw materials.

Materials	Composition (wt%)							
	MgO	Al <sub>2</sub> O <sub>3</sub>	SiO <sub>2</sub>	K <sub>2</sub> O	CaO	Fe <sub>2</sub> O <sub>3</sub>	SO <sub>3</sub>	Other
OPC	1.21	5.67	18.43	0.32	63.04	3.09	2.51	5.73
Sand	0.01	2.04	95.52	0.24	0.15	1.01	0.18	0.85
Gypsum	0.20	0.15	0.14	0.05	24.61	0.10	73.12	1.63

Calcium silicate hydrate (C-S-H) is the product from hydration reaction of Portland cement. According to John *et al* [28], the C-S-H powder can be used as the admixture for accelerating the hydration reaction. Tobermorite is the crystalline phase of C-S-H normally found when FRCC are cured by the autoclave. As shown in our previous works, the morphology of tobermorite affects the mechanical properties and the physical properties of FRCC such as improving strength or reduced water absorption [15]. Wang *et al* [29] found that tobermorite could be synthesized using the synthetic tobermorite as the precursor.

As mentioned before, reduction of the energy used in the manufacturing process is an approach to reduce the carbon-footprint of FRCC and using the chemical admixture could enhance the chemical reaction within the concrete. Therefore, the objective of this work was to develop a FRCC samples by lowering embodied energy via the moisture curing process by using the crystal modifiers (CM), a group of chemical admixtures, including a modified lithium compound, alumino-silicate complex, and synthetic tobermorite as the additives to enhance the chemical reaction of the cement. The effect of each CM on the rate of hydration reaction was compared based on the method described in ASTM C186-98 standards [30]. Moreover, the mechanical and physical properties of the fiber-cement samples were characterized based on ASTM C1185 standards [31]. Scanning electron microscope (SEM) was used to observe the microstructure of samples.

## 2. Experimental

### 2.1 Materials

The raw materials used in this work were ordinary Portland cement (OPC), sand, gypsum, cellulose fiber, and the crystal modifiers (CM) which were the admixtures used to modify the crystalline phase in FRCC. Three types of CM were used including:

CM1: modified lithium compound which was the lithium-based zeolite prepared from chemisorption of lithium carbonate on synthetic zeolite.

CM2: alumino-silicate complex which was prepared by heat treatment of agro-waste ash and recycle concrete mixtures and

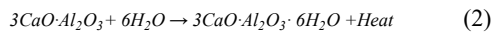
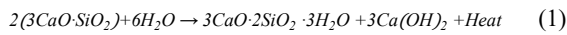
CM3: synthetic tobermorite which was prepared by the precipitation process from the aqueous solutions of sodium silicate (Na<sub>2</sub>SiO<sub>3</sub>) and calcium nitrate (Ca(NO<sub>3</sub>)<sub>2</sub>).

These CM were supplied by and under the licensing agreement of Shera Public Company Limited.

X-ray fluorescence spectrometer (XRF, Panalytical-Minipal 4) were used to determine the chemical composition of OPC, sand, and gypsum, shown in Table 1.

## 2.2 Reaction Rate of Hydration Reaction

The effect of CM on the reaction rate of hydration reaction was determined using the method based on ASTM C186-98 standards [30]. The water and OPC were mixed with water to cement (w/c ratio) of 0.35. Then CM was added at the amount of 0% to 6% of OPC weight. The mixtures were kept in the chamber of the instrument. The heat generated due to the exothermic reaction of chemical components inside OPC, such as the reaction shown in Equation (1-2) was observed through the temperature change within the chamber. According to Equation (1), tricalcium silicate ( $3CaO \cdot SiO_2$ ) reacts with water, which generates heat and produces calcium silicate hydrate ( $3CaO \cdot 2SiO_2 \cdot 3H_2O$ , CSH) and calcium hydroxide ( $Ca(OH)_2$ , CH) as the products. [32,33] For another reaction, from Equation (2), tricalcium aluminate ( $3CaO \cdot Al_2O_3$ ) reacts with water to form calcium aluminate hydrate ( $3CaO \cdot Al_2O_3 \cdot 6H_2O$ , CAH) [34].



From our previous work [6], the average rate of the temperature change (R) from initial temperature ( $T_{initial}$ ) to maximum temperature ( $T_{max}$ ) during the time t is

$$R = \frac{T_{max} - T_{initial}}{t} \quad (3)$$

## 2.3 Fiber-cement samples preparation and characterization

The mix proportion for preparing the samples, OPC, sand, gypsum, and cellulose fibers were first mixed with water, shown in Table 2. After mixing as needed the CM was added, then the fiber-cement samples were produced by a filter pressing machine. For curing, the samples without the addition of CM were either cured in air for 8 h. and then placed in an autoclave at 180°C and 10 bar for 16 h or only cured in air by keeping the samples in the closed chamber for 1 day at 70°C, ambient pressure, and 95% relative humidity. The former method will be called “autoclave curing”, and the latter method will be called “moisture curing”. Moisture curing was only applied to the samples with CM additions.

After curing for 1 day, the properties including modulus of rupture (MOR), modulus of elasticity (MOE), bulk density, and % water absorption were determined by the methods described in ASTM C1185 standards [31]. Mechanical tests used a Instron 3300-series universal testing machine, each material has 10 samples providing statistics. The Archimedes’ method determined the bulk density and % water absorption of the samples calculated by:

$$Bulk\ Density = \frac{W_d}{W_w - W_s} \quad (4)$$

$$\% \text{ Water Absorption} = \frac{W_w - W_d}{W_d} \times 100 \quad (5)$$

where  $W_d$ ,  $W_w$  and  $W_s$  are the weights of the dry sample, sample suspended in the water, and sample just removed from the water, respectively. Moreover, the microstructure of the cured samples was observed by scanning electron microscope (SEM, FEI Quanta 450).

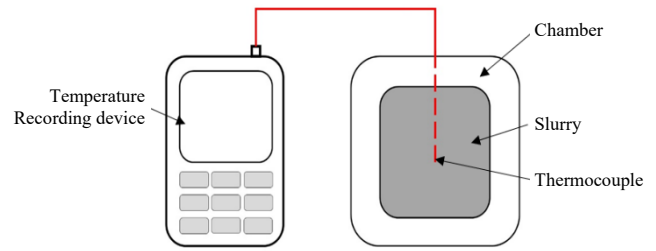


Figure 1. Schematic representation of the instrument for heat of hydration measurement.

Table 2. Composition for preparing the fiber-cement samples.

Materials (wt%)				
OPC	Sand	Gypsum	Cellulose fibers	CM (CM1, CM2, or CM3) (% of OPC weight)
42.5	42.5	10	5	0-6

## 3. Results and discussion

### 3.1 Reaction rate of hydration reaction

Results from heat of hydration test, Figure 2, where REF represents the OPC/water mixture contain 0% crystal modifier. Additionally, the initial temperature ( $T_{initial}$ ), maximum temperature ( $T_{max}$ ), and the time (t) to reach the maximum temperature are listed in Table 3. Using these data, the average rate of the temperature change (R) for each CM was calculated using Equation 1. The results are presented in Figure 3 as the relative value of the  $R_i/R_r$  ratio when  $R_i$  and  $R_r$  are the average rate of the temperature change with and without using a CM. Thus the  $R_i/R_r$  ratio represents the effectiveness of each CM, section 2.1, amount on the enhancement of hydration reaction.

Because the values of the  $R_i/R_r$  ratio are greater than 1 in all cases, using these CM enhances the reaction rate of hydration process. The ratio of  $R_i/R_r$  increases with the increasing of amount of CM, between 1% to 6 % of OPC weight, Figure 3. Hence, increasing of either CM1 or CM2 will improve the rate of hydration reaction. Because the slope of the trendline, Figure 2(a) is greater than that of Figure 2(b), therefore addition of CM1 had a more pronounced effect on the reaction kinetic than CM2.

Obviously, zeolite in CM1, and the crystal modifier CM2 are alumino-silicate compound. The improved in hydration reaction rate should be from the pozzolanic reaction of CH from hydration reaction in Equation (1) with  $SiO_2$  and  $Al_2O_3$  of zeolite in CM1, and the crystal modifier CM2 which yield CSH and  $3CaO \cdot Al_2O_3 \cdot 6H_2O$  as shown below [35] :



According to Song, *et al* [18], CSH could be a product from the chemical reaction between lithium silicate ( $Li_2O \cdot nSiO_2$ ) with CH as shown in Equation (6).



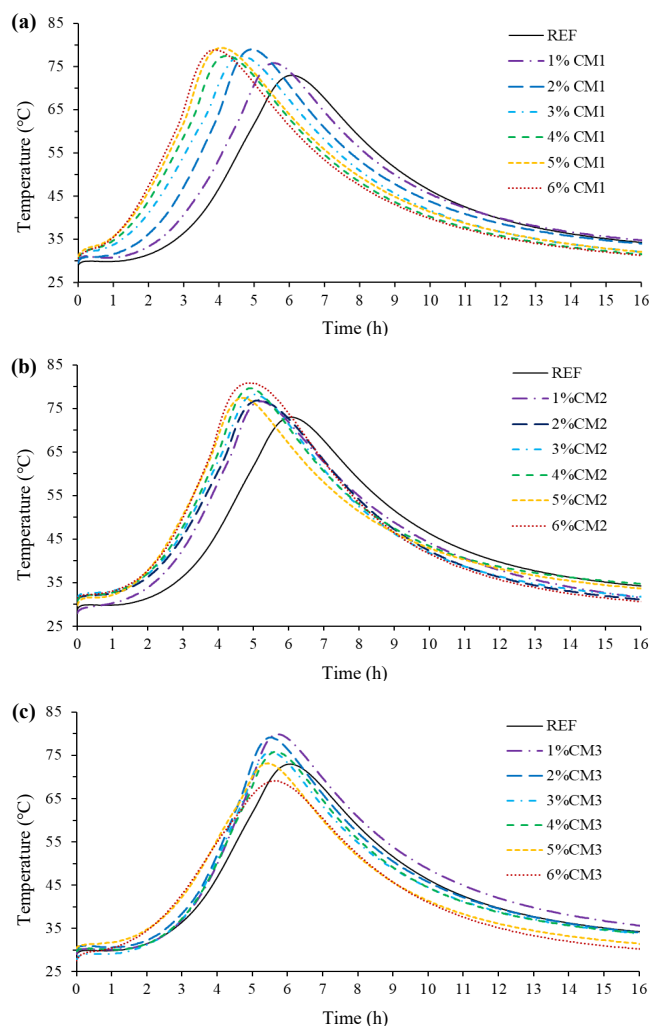
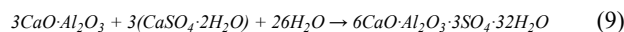


**Figure 2.** The results from heat of hydration test when (a) CM1 (b) CM2 and (c) CM3 were used as the chemical admixture.

**Table 3.** Numerical results from heat of hydration test used.

CM	Amount of CM (% OPC weight)	T <sub>initial</sub> (°C)	T <sub>max</sub> (°C)	t (h:min)	R (°C·h <sup>-1</sup> )	R <sub>i</sub> /R <sub>r</sub>
REF	0	28.93	73	06:05	7.24	1.00
CM1	1	29.7	75.8	05:31	8.36	1.15
	2	29.5	79	04:54	10.10	1.39
	3	30.4	77.4	04:34	10.29	1.42
	4	30.7	77.5	04:11	11.19	1.54
	5	31.1	79.3	03:59	12.10	1.67
	6	30.6	78.8	03:47	12.74	1.76
CM2	1	27.9	76.7	05:12	9.38	1.30
	2	30.8	76.9	05:08	8.98	1.24
	3	28.6	78.2	04:58	9.99	1.38
	4	27.6	79.6	04:51	10.72	1.48
	5	29.8	77.4	04:38	10.27	1.42
	6	28.0	80.9	04:53	10.83	1.50
CM3	1	29.1	79.9	05:42	8.91	1.23
	2	29.8	79.1	05:27	9.05	1.25
	3	27.7	75.8	05:29	8.77	1.21
	4	29.7	75.8	05:36	8.23	1.14
	5	30.4	73.2	05:26	7.88	1.09
	6	27.6	69.1	05:33	7.48	1.03

Normally, the hydration reaction of  $3\text{CaO}\cdot\text{Al}_2\text{O}_3$  according to Equation (2) has a high reaction rate, resulting in quick setting time of the cement. To delay cement setting process, the cement manufacturer will add gypsum ( $\text{CaSO}_4\cdot 2\text{H}_2\text{O}$ ) to the clinker when cement is made. From Equation (9), the delay of cement setting occurs by the reaction between  $3\text{CaO}\cdot\text{Al}_2\text{O}_3$  from the cement with  $\text{CaSO}_4\cdot 2\text{H}_2\text{O}$  which produce ettringite ( $6\text{CaO}\cdot\text{Al}_2\text{O}_3\cdot 3\text{SO}_3\cdot 32\text{H}_2\text{O}$ ) over the surface of cement particles.



According to Witzleben [36], the lithium aluminum hydroxide compound ( $\text{Li}[\text{Al}(\text{OH})_4]$ ) could prevent ettringite formation, resulting in the increasing of hydration rate from  $3\text{CaO}\cdot\text{Al}_2\text{O}_3$ .

Thus, the enhanced rate of hydration reaction by CM1 and CM2 could be from the pozzolanic reaction as shown in Equation (6-7). As mentioned before, CM1 is more effective than CM2. This could be from  $\text{Li}_2\text{O}$ ,  $\text{SiO}_2$ , and  $\text{Al}_2\text{O}_3$  in CM1 which produce the additional CH as shown in Equation (8), or prevent ettringite formation from the reaction between  $3\text{CaO}\cdot\text{Al}_2\text{O}_3$  and  $\text{CaSO}_4\cdot 2\text{H}_2\text{O}$  as shown in Equation (9).

For CM3, Figure 2(c), when the amount of CM3 is over 2% of OPC weight, there is a reduction of  $R_i/R_r$  ratio. According to He *et al* [37], calcium silicate hydrate, a product from hydration reaction as shown in Equation (1), could nucleate on the surface of cement particles and also on the surface of CM3 for our case. Referring to Zhou *et al* [38], the impingement of the particle used as the nucleation site for calcium silicate hydrate could reduce the hydration reaction rate. Therefore, the reduction in effectiveness of CM3, when the amount was over 2% of OPC weight, should be from the CM3-particle impingement which reduce the surface area for calcium silicate hydrate nucleation.

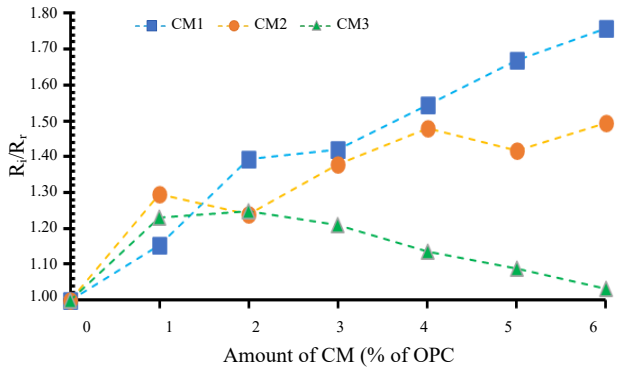


**Figure 3.** The relative rate of temperature change of by using CM1, CM2, and CM3.

### 3.2 Mechanical and physical properties

The results from mechanical test including MOR and MOE are shown in Figure 4(a-b). The dash lines on both figures represent the minimum requirement from the fiber-cement industry. The REF represents the fiber-cement samples without adding a CM. As mentioned in section 2.3, REF samples were cured by either autoclave curing or moisture curing. Apparently, while the MOR and MOE of autoclave-cured REF samples passed the industry requirements, moisture-cured REF samples did not. However, when a CM was added, MOR and MOE of all CM-added samples satisfied the industrial requirements. For CM-added samples, MOE are higher than MOE of autoclave-cured samples when CM1 or CM2 were utilized. Moreover, among the CM-added samples, MOR and MOE were highest when CM2 was used at 3% of OPC weight.

The bulk density and the % water absorption of the fiber-cement samples are shown in Figure 5(a-b). When CM2 was used at 3% of OPC weight, bulk density of the samples was highest. % water absorption of the CM-added samples was lower than that of both autoclave and moisture-cured REF samples. As mentioned in the previous work, a lower degree of water absorption is the favorable feature especially for outdoor applications [13].

In the SEM micrographs (Figure 6) of the samples, for the CM-added samples, the amount of CM was 3% of OPC weight. Plate-shape tobermorite is a product of the autoclave-cured REF samples (Figure 6(a)). Obviously, tobermorite is not found in the moisture-cured REF samples (Figure 6(b)) but are found in the CM-added samples, and they have needle shape (Figure 6(c-e)), similar to our previous work [7,39] and the works by Komarneni *et al* [40], Liu *et al* [41], and Ding *et al* [42].

Therefore, the combination of moisture curing, and CM promoted the nucleation of tobermorite at the ambient pressure. According to Maeda *et al* [43] and Majdinasab *et al* [44], larger aluminum content could produce larger crystal of tobermorite. Because CM2 has high aluminum content, the size of needle-shape tobermorite phase is relatively largest when CM2 was applied as shown on Figure 6(d).

From the previous work [28], the amount of reinforcement phase affects the MOE of FRCC. In this work, the percentage of cellulose fibers in each sample is similar. Therefore, the improved MOE of CM-added samples should be from the improved MOE of cement matrix from the forming of needle-shape tobermorite phase especially when

CM1 and CM2 were used. Moreover, compared with Figure 6(a), the arrangement of the small needle-shape tobermorite in Figure 6(c-e) improves bulk density and reduce the capillary action of water resulting in the reduction of % water absorption.

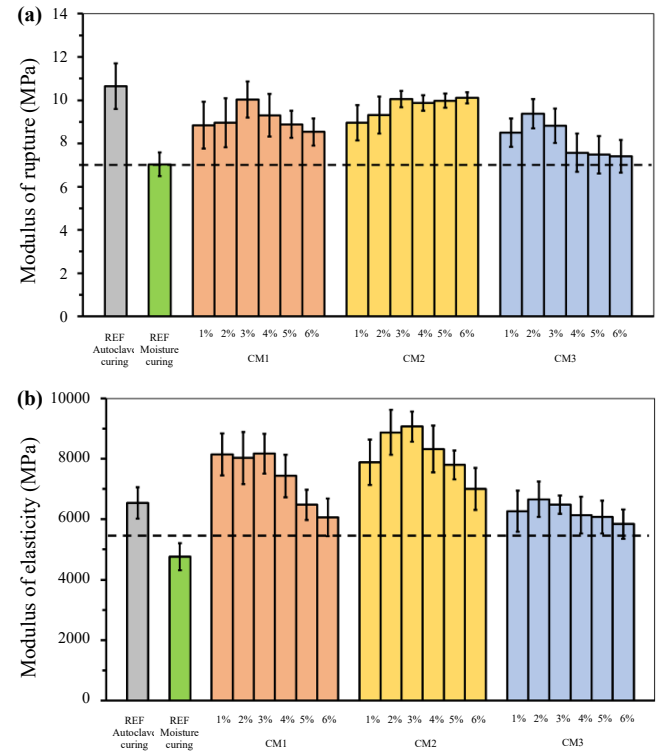


**Figure 4.** Mechanical properties of fiber-cement samples (a) MOR and (b) MOE.

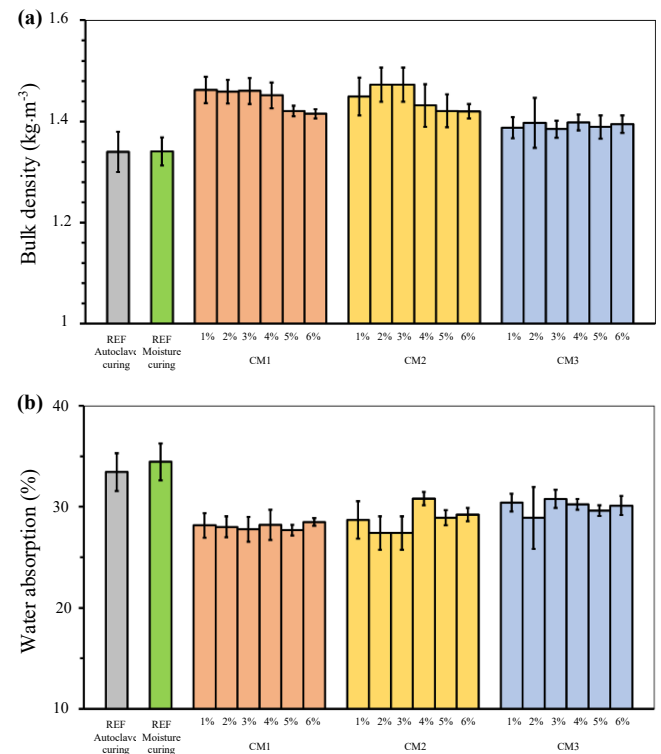


**Figure 5.** Properties of fiber-cement samples (a) bulk density and (b) % water absorption.

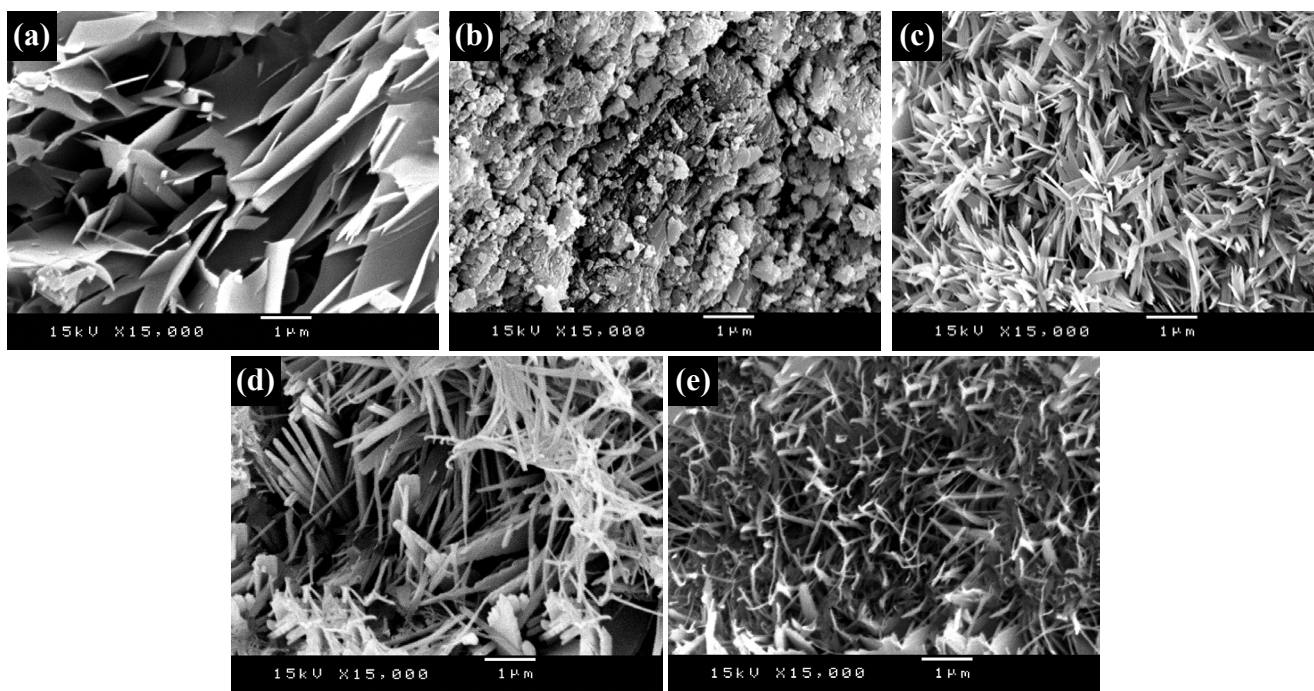


**Figure 6.** Scanning electron micrographs of samples taken at 15000x magnification, (a) autoclave curing, (b) moisture curing without CM, (c) CM1, (d) CM2, and (e) CM3. The amount of CM in all cases was 3% of OPC weight.

#### 4. Conclusions

The purpose of this work was to develop fiber-reinforced cement composites with an extremely low embodied energy by using moisture curing with a crystal modifier (CM). Three types of CM crystal modifier were used including: modified lithium compound, alumino silicate complex, and synthetic tobermorite. The results indicated that

- The utilization of CM with low embodied energy curing process could produce the fiber-cement products having the mechanical properties as required by the industry
- The mechanical properties of the fiber-cement products were improved by the CM.
- Compared with autoclave curing, using alumino-silicate complex as the CM at 3% of OPC weight yield the highest modulus of elasticity and the lowest % water absorption.

Bio-circular-green or a BCG economy model is proposed by the Thai government to improve the industrial sector, and a tool for the economic recovery after the pandemic. Based on this economic model, reduction of carbon-footprint or achieving net zero greenhouse gas emissions are part of the Thai government plan. In this work, fiber-reinforced cement composites with an extremely low embodied energy by using moisture curing with a CM, have mechanical properties that exceeds industry standards, reducing energy reequipments and cost and a significant reduction of the carbon-footprint in fiber-cement product production, supporting the environmental policy of the country.

For the construction materials market, price is still considered as the order qualifier, a factor that causes the consumer to consider purchase of items. However, for many consumers, low environmental impacts are the most important factor to a consumer's final decision on purchasing items.

#### Acknowledgements

This work was supported by Faculty of Engineering, Kasetsart University [Grant No. 63/02/D.Eng], and Shera Public Company Limited.

#### References

- [1] National News Bureau of Thailand. "PM tells world leaders: Thailand will step up fight against climate change." <https://thainews.prd.go.th/en/news/detail/%20TCATG211102174518827> (accessed 2022).
- [2] The Office of Natural Resources and Environmental Policy and Planning (ONEP). "Greenhouse Gas Inventory Report: Manufacturing Processes and Product Uses." [https://climate.onep.go.th/wpcontent/uploads/2020/02/Meeting\\_document\\_4.1.pdf](https://climate.onep.go.th/wpcontent/uploads/2020/02/Meeting_document_4.1.pdf) (accessed Dec, 2021).
- [3] Intergovernmental Panel on Climate Change, "2006 IPCC Guidelines for National Greenhouse Gas Inventories," in *Industrial Processes and Product Use*, vol. 3, 2006.
- [4] P. González-Vallejo, M. Marrero, and J. Solís-Guzmán, "The ecological footprint of dwelling construction in Spain," *Ecological Indicators*, vol. 52, pp. 75-84, 2014.
- [5] N. Kongkajun, E. A. Laitila, P. Ineure, W. Prakaypan, B. Cherdhirunkorn, and P. Chakartnarodom, "Soil-cement bricks produced from local clay brick waste and soft sludge from fiber cement production," *Case Studies in Construction Materials*, vol. 13, 2020.
- [6] P. Sonprasarn, P. Chakartnarodom, P. Ineure, and W. Prakaypan, "Effects of the chemical treatment on coal-fired bottom ash

- for the utilization in fiber-reinforced cement," *Journal of Metals, Materials and Minerals*, Article vol. 29, no. 4, pp. 55-60, 2019, doi: 10.14456/jmmm.2019.47.
- [7] P. Sonprasarn, P. Chakartnarodom, N. Kongkajun, and W. Prakaypan. Microstructure and mechanical performance of fiber-reinforced cement composites made with nucleating-agent activated coal-fired power plant bottom ash, *Solid State Phenomena*, vol. 302 SSP, pp. 85-92, 2020.
- [8] P. Pahuswanno, P. Chakartnarodom, P. Ineure, and W. Prakaypan, "The influences of chemical treatment on recycled rejected fiber cement used as fillers in the fiber cement products," *Journal of Metals, Materials and Minerals*, Article vol. 29, no. 3, pp. 66-70, 2019, doi: 10.14456/jmmm.2019.36.
- [9] P. Pahuswanno, P. Chakartnarodom, N. Kongkajun, and W. Prakaypan. Feasibility study of using modified recycled fiber-cement for the production of high performance fiber-cement composites, *Solid State Phenomena*, vol. 302 SSP, pp. 93-99, 2020.
- [10] A. M. Zeyad, B. A. Tayeh, A. Adesina, A. R. G. de Azevedo, M. Amin, M. Hadzima-Nyarko, and I. S. Agwa, "Review on effect of steam curing on behavior of concrete," *Cleaner Materials*, vol. 3, p. 100042, 2022.
- [11] D. R. Askeland, P. P. Fulay, and W. J. Wrigh, *The Science and Engineering of Materials*, sixth ed. Stamford, CT Cengage Learning, 2011.
- [12] P. Chakartnarodom, W. Prakaypan, P. Ineure, N. Kongkajun, and N. Chuankrerkkul, "Formula of basalt fiber-reinforced cement board," Thailand Patent 12440, 2017. [Online]. Available: [https://patentsearch.ipthailand.go.th/DIP2013/view\\_public\\_data.php?appno=11623600023](https://patentsearch.ipthailand.go.th/DIP2013/view_public_data.php?appno=11623600023)
- [13] P. Chakartnarodom, W. Prakaypan, P. Ineure, N. Kongkajun, and N. Chuankrerkkul, "Formula of basalt fiber-reinforced roof tiles," Thailand Patent 15370, 2019. [Online]. Available: [https://patentsearch.ipthailand.go.th/DIP2013/view\\_public\\_data.php?appno=11623600023](https://patentsearch.ipthailand.go.th/DIP2013/view_public_data.php?appno=11623600023)
- [14] P. Chakartnarodom, W. Prakaypan, P. Ineure, N. Kongkajun, and N. Chuankrerkkul, "Formula of basalt fiber-reinforced roof-tiles cover " Thailand Patent 18025, 2021. [Online]. Available: [https://patentsearch.ipthailand.go.th/DIP2013/view\\_public\\_data.php?appno=11623600023](https://patentsearch.ipthailand.go.th/DIP2013/view_public_data.php?appno=11623600023)
- [15] P. Chakartnarodom, N. Kongkajun, N. Chuankrerkkul, P. Ineure, and A. W. Prakaypan, "Reducing water absorption of fiber-cement composites for exterior applications by crystal modification method," *Journal of Metals, Materials and Minerals*, Article vol. 29, no. 4, pp. 90-98, 2019.
- [16] P. Chakartnarodom, W. Prakaypan, P. Ineure, N. Kongkajun, and N. Chuankrerkkul. *Feasibility study of using basalt fibers as the reinforcement phase in fiber-cement products*, *Key Engineering Materials*, vol. 766 KEM, pp. 252-257, 2018.
- [17] P. Chakartnarodom, W. Prakaypan, P. Ineure, N. Chuankrerkkul, E. A. Laitila, and N. Kongkajun, "Properties and performance of the basalt-fiber reinforced texture roof tiles," *Case Studies in Construction Materials*, vol. 13, p. e00444, 2020.
- [18] Z. Song, Z. Lu, and Z. Lai, "The effect of lithium silicate impregnation on the compressive strength and pore structure of foam concrete," *Construction and Building Materials*, vol. 277, p. 122316, 2021.
- [19] Z.-h. He, S.-g. Du, and D. Chen, "Microstructure of ultra high performance concrete containing lithium slag," *Journal of Hazardous Materials*, vol. 353, pp. 35-43, 2018.
- [20] S. O. Ekolu, M. D. A. Thomas, and R. D. Hooton, "Dual effectiveness of lithium salt in controlling both delayed ettringite formation and ASR in concretes," *Cement and Concrete Research*, vol. 37, no. 6, pp. 942-947, 2007.
- [21] F. Dabbaghi, A. Sadeghi-Nik, N. A. Libre, and S. Nasrollahpour, "Characterizing fiber reinforced concrete incorporating zeolite and metakaolin as natural pozzolans," *Structures*, vol. 34, pp. 2617-2627, 2021
- [22] S. Ganji, H. E. Sharabiani, and F. Zeinali, "Laboratory investigation on abrasion resistance and mechanical properties of concretes containing zeolite powder and polyamide tire cord waste as fiber," *Construction and Building Materials*, vol. 308, p. 125053, 2021
- [23] X. Zheng, J. Zhang, X. Ding, H. Chu, and J. Zhang, "Frost resistance of internal curing concrete with calcined natural zeolite particles," *Construction and Building Materials*, vol. 288, p. 123062, 2021.
- [24] M. Tayebi and M. Nematzadeh, "Post-fire flexural performance and microstructure of steel fiber-reinforced concrete with recycled nylon granules and zeolite substitution," *Structures*, vol. 33, pp. 2301-2316, 2021
- [25] P. V. Madhuri, B. Kameswara Rao, and A. Chaitanya, "Improved performance of concrete incorporated with natural zeolite powder as supplementary cementitious material," *Materials Today: Proceedings*, vol. 47, pp. 5369-5378, 2021.
- [26] M. H. Zhang and V. M. Malhotra, "Characteristics of a thermally activated alumino-silicate pozzolanic material and its use in concrete," *Cement and Concrete Research*, vol. 25, no. 8, pp. 1713-1725, 1995.
- [27] N. M. Al-Akhras, "Durability of metakaolin concrete to sulfate attack," *Cement and Concrete Research*, vol. 36, no. 9, pp. 1727-1734, 2006.
- [28] E. John, J. D. Epping, and D. Stephan, "The influence of the chemical and physical properties of C-S-H seeds on their potential to accelerate cement hydration," *Construction and Building Materials*, vol. 228, p. 116723, 2019.
- [29] S. Wang, X. Peng, L. Tang, L. Zeng, and C. Lan, "Influence of inorganic admixtures on the 11Å-tobermorite formation prepared from steel slags: XRD and FTIR analysis," *Construction and Building Materials*, vol. 60, pp. 42-47, 2014.
- [30] *ASTM C186-98 Standard Test Method for Heat of Hydration of Hydraulic Cement*, ASTM International, West Conshohocken, PA, USA.
- [31] *ASTM C1185 Standard Test Methods for Sampling and Testing Non-Asbestos Fiber-Cement Flat Sheet, Roofing and Siding Shingles, and Clapboards*, ASTM International, West Conshohocken, PA, USA, 2016.
- [32] V. Dwivedi, S. Das, N. Singh, S. Rai, and N. Gajbhiye, "Portland cement hydration in the presence of admixtures -

- Black gram pulse and superplasticizer," *Materials Research-ibero-american Journal of Materials - MATER RES-IBERO-AM J MATER*, vol. 11, 2008.
- [33] P. Chakartnarodom, W. Prakaypan, P. Ineure, N. Kongkajun, and N. Chuankrerkkul, "Feasibility study of using basalt fibers as the reinforcement phase in fiber-cement products," *Key Engineering Materials*, vol. 766, pp. 252-257, 2018.
- [34] G. C. Bye, P. Livesey, and L. J. Struble, *Portland Cement*. Institution of Civil Engineers Publishing, 2011.
- [35] Y. T. Tran, J. Lee, P. Kumar, K.-H. Kim, and S. S. Lee, "Natural zeolite and its application in concrete composite production," *Composites Part B: Engineering*, vol. 165, pp. 354-364, 2019.
- [36] S. T. Witzleben, "Acceleration of Portland cement with lithium, sodium and potassium silicates and hydroxides," *Materials Chemistry and Physics*, vol. 243, p. 122608, 2020.
- [37] D. Marchon, and R. J. Flatt, "8 - Mechanisms of cement hydration," in *Science and Technology of Concrete Admixtures*, P.-C. Aïtcin and R. J. Flatt Eds.: Woodhead Publishing, 2016, pp. 129-145.
- [38] W. Zhou, L. Duan, S. Tang, E. Chen, and A. Hanif, "Modeling the evolved microstructure of cement pastes governed by diffusion through barrier shells of C-S-H," *Journal of Materials Science*, 2019.
- [39] P. Chakartnarodom, N. Kongkajun, N. Chuankrerkkul, P. Ineure, and W. Prakaypan, "Reducing water absorption of fiber-cement composites for exterior applications by crystal modification method," *Journal of Metals, Materials and Minerals*, vol. 29, no. 4, pp. 90-98, 2019.
- [40] S. Komarneni, M. Miyake, and R. Roy, "Cation-exchange properties of (Al + Na)-substituted synthetic tobermorites," *Clays and Clay Minerals - CLAYS CLAY MINER*, vol. 35, pp. 385-390, 1987.
- [41] Y. Liu, B. Leong, Z.-T. Hu, and E.-H. Yang, "Autoclaved aerated concrete incorporating waste aluminum dust as foaming agent," *Construction and Building Materials*, vol. 148, pp. 140-147, 2017.
- [42] J. Ding, Z. Tang, S. Ma, Y. Wang, S. Zheng, Y. Zhang, S. Shen, and Z. Xie, "A novel process for synthesis of tobermorite fiber from high-alumina fly ash," *Cement and Concrete Composites*, vol. 65, pp. 11-18, 2016.
- [43] H. Maeda, A. Kazuki, and H. Ishida, "Hydrothermal synthesis of aluminum substituted tobermorite by using various crystal phases of alumina," *Journal of the Ceramic Society of Japan*, vol. 119, pp. 375-377, 2011.
- [44] A. Majdinasab, and Q. Yuan, "Synthesis of Al-substituted 11Å tobermorite using waste glass cullet: A study on the microstructure," *Materials Chemistry and Physics*, vol. 250, p. 123069, 2020.